EGG Objective characterization of cybersickness symptoms towards navigation axis

Nana Tian* Khalil Haroun Achache† Ali Raed Ben Mustapha‡ Ronan Boulic§

École Polytechnique Fédérale de Lausanne
Lausanne, Swizerland

ABSTRACT

The current study sought to objectively evaluate cybersickness by utilizing Electrogastrogram (EGG) physiological data in relation to three different navigation axes: Translational movement along the longitudinal and lateral axes, and rotation along the vertical Yaw axis. EGG was employed as it has been clinically identified as a valuable tool for capturing dysfunction in the stomach. This resulted in a 2x2x2 factorial design. Results from both subjective and objective measurements (N=26, F=10) indicate that rotation along the Yaw axis is the primary factor influencing cybersickness. Additionally, it was found that individuals who are not susceptible to cybersickness do not exhibit any dominant factors.

In summary, through the analysis of EGG data, several key physiological indicators of individual susceptibility to cybersickness were identified. The findings suggest that there is a positive correlation between the mean dominant frequency and the tachygastria ratio with individual susceptibility, while the normalgastria and normaltachy ratio were found to be negatively correlated with individual susceptibility

1 INTRODUCTION

The phenomenon of cybersickness remains a significant challenge that hinders the widespread adoption of virtual reality technology. Researchers have proposed various theories to explain this complex issue. One such theory is the sensory conflict theory, which posits that a mismatch between the vestibular and visual senses may lead to motion sickness. This theory suggests that the level of motion sickness is positively correlated with the magnitude of the mismatch [23]. While this theory provides insight into the potential neural mechanisms of motion sickness, it does not fully account for individual differences in susceptibility [33].

Recently, the postural instability theory has been extensively examined as a potential explanation for cybersickness [3, 4, 36]. This theory attributes motion sickness to an individual's inability to maintain postural stability [24]. The key assumption is that the level of motion sickness is linked to an individual's capacity to control their body posture [33]. Studies have intensively measured postural instability as a symptom of disorientation in recent years [3, 18], however, this measure was not adopted in the current study. This is due to several reasons: first, postural instability measures are most applicable in applications that require a standing posture, whereas many applications such as the 3D game in this study are performed in a seated position. Second, previous studies have indicated that standing is more sickness-inducing than sitting, thus, adopting a standing posture would increase the likelihood of participants prematurely ending the experiment and introducing random movement noise. Third, fewer studies have explored nausea symptoms.

The issue of individual susceptibility in cybersickness has recently gained significant attention in the literature [7, 21, 28]. However, most discussions have focused on factors such as gender or age, while the frequently observed phenomenon of individuals exhibiting different sensitivities to various factors or combinations of factors [31]is often under-explored.

For example, a study by Lo et al. [19] attempted to understand the influence of three isolated rotational axes (Yaw, Pitch, and Roll) on cybersickness and found that there was no dominant cybersickness-inducing axis. However, a more recent study [22] has shown that rotation around the front-to-back axis (Roll) has a stronger influence than the other two axes. Additionally, some studies have found that rotation around the side-to-side axis (Pitch) can induce sickness symptoms faster than rotation around the vertical axis (Yaw) [12, 30]. The differences in these findings may be attributed to factors such as rotation magnitude, rotation patterns, duration of virtual reality exposure, and, most importantly, individual susceptibility to different factors.

The symptoms of cybersickness, also known as simulator sickness, that individuals may experience during exposure to virtual reality (VR) content can range from eye fatigue to severe nausea. The Simulator Sickness Questionnaire (SSQ) [23] is the most widely accepted standardized subjective measure of cybersickness and identifies three main symptoms: disorientation, oculomotor, and nausea. However, subjective measures have been found to lack reliability compared to objective measures [20]. Additionally, subjective measures may not be robust enough to accurately quantify individual susceptibility, as ratings may not be calibrated in a consistent manner between individuals.

Objective physiological signals have been investigated as a potential means of assessing individual cybersickness, with a focus on nausea symptoms. However, the interpretation of such signals is generally more complex and results of studies in this area have been inconsistent. The present study aims to clarify the potential of Electrogastrogram (EGG) physiological signals for assessing individual cybersickness.

Electrogastrography (EGG) is a non-invasive technique for assessing gastric myoelectrical activity using surface electrodes with conductive gel applied to the stomach [26]. The normal EGG frequency for healthy individuals in a fasting state is three cycles per minute (3 cpm) within a broad range of 2-4 cpm [2, 26]. The normal EGG ratio represents the proportion of EGG dominant frequencies that fall within this normal range, and for healthy individuals, this ratio is typically above 70 percent or even higher [25]

EGG signals have been clinically shown to be capable of detecting stomach motor dysfunctions, particularly dysrhythmias such as tachygastria (0.5-2 cpm) or bradygastria (4-9 cpm) (Koch, 2014; Chen, 1991; Yin, 2013). However, only a few studies have used EGG to detect cybersickness (Kim, 2005; Farmer, 2015). In the context of cybersickness, an increase in tachygastria has been reported (Kim, 2005; Farmer, 2015; Dennison, 2016), while a decrease in bradygas-

*nana.tian@epfl.ch
†khalil.acheche@epfl.ch
‡ali.benmustapha@epfl.ch
§e-mail:ronan.boulic@epfl.ch

\copyright 2023 IEEE. Personal use of this material is permitted. Permission from IEEE must be obtained for all other uses, in any current or future media, including reprinting/republishing this material for advertising or promotional purposes, creating new collective works, for resale or redistribution to servers or lists, or reuse of any copyrighted component of this work in other works.
https://ieeexplore.ieee.org/document/10108555

tria was reported in (Dennison, 2016). It is worth noting that only Dennison et al. used true VR systems to induce cybersickness, and the reporting of a large bradygastria ratio (above 70 percent) in the resting state was in violation of previous studies that claimed that normalgastria ratio should be dominant in healthy participants. This discrepancy may be due to calculation errors or non-cleaned signals.

The contributions of this study are three-fold: to investigate whether there exists a dominant factor or combination of factors that contribute to cybersickness for each individual, to provide an objective characterization of cybersickness using Electrogastrography (EGG) data and to investigate the parameters of EGG. Additionally, the experiment design was deliberately crafted to re-evaluate prior findings in the relevant literature. To that end, a comprehensive set of data analyses was carried out.

The experimental design, including the full-factorial approach, and the details of the EGG data processing are presented in the following sections. Then the results of the study are described, followed by a discussion and conclusion.

2 Experiment Design

This study is a full factorial design with the longitudinal axis, the lateral axis and yaw axis as three within-subject factors. **The selection of these factors is based upon their prevalence as navigation axes within virtual reality gaming contexts**. The longitudinal factor (short as 'X' in the later context) has two levels: 1) **Has no translational movement** 2) **Has translational movement**. Similarly, the lateral axis factor (short as 'Z' in the later context) has two levels: 1) **Has no translational movement** 2) **Has translational movement**. Lastly, the yaw axis (short as 'R' in the later context) also has two levels: 1) **Has no rotational movement** 2) **Has rotational movement**. Overall, this eventually yields a 2*2*2 factorial design, with the following combinations where the letter **o** indicates no movement along the axis in the (X,Z,R) combination: **'ooo','xoo','ozo', 'xzo', 'oor', 'xor','ozr', 'xzr'.**

2.1 Game design

In order to maintain the quality of the physiological recordings and minimize the potential impact of individual differences related to navigation control, the displacements within the virtual environment were pre-programmed. Additionally, to ensure that the participant remained engaged and in the "game flow" [29] during the VR experience, minimal game interactions were implemented, requiring the use of a controller to extinguish fires on buildings along the path. The player's view within the game is illustrated in Figure 1. A supplementary video is also provided to further demonstrate the gameplay experience.

2.2 Condition description

- **ooo condition:** in the ooo condition, there is no movement in the scene, the participants can use the controller to extinguish the fire in the buildings in front of them.
- **xoo condition:** in the xoo condition, the movements are constrained in the longitudinal axis (forward and backward) within a limited range. The movement follows a forward-backward repetitive pattern with a change of speed on a fixed time interval (10s).
- **ozo condition:** in the ozo condition, the movements are constrained in the lateral axis (left and right direction) within a limited range (the same path as in the xoo condition but the user was rotated 90 degrees on the yaw axis to move left and right instead). The movement follows a forward-backward repetitive pattern with a change of speed on a fixed time interval (10s).
- **xzo condition:** in the xzo condition, the movements are constrained in the longitudinal and lateral axis within a limited range (the path is extended to a rectangular shape). Again, the movement follows a forward-backward repetitive pattern with a change of speed on a fixed time interval (10s).
- **oor condition:** in the oor condition, there is no translation movement but only rotational movement along the yaw axis. The user rotates left and right during a 10 seconds interval with an angle randomly picked between (30°, 150°, 210°, 330°).
- **xor condition:** in the xor condition, there is a combination of a translation movement on the longitudinal axis and a rotational movement along the yaw axis.The periodic change of speed happens simultaneously on both the axis at the fixed time interval as above. The speed, acceleration and rotation profile are the same as above.
- **ozr condition:** in the ozr condition, there is a combination of a translation movement on the lateral axis and rotational movement along the yaw axis, similar to the xor condition.
- **xzr condition:** in the xzr condition, there is a combination of translational on both longitudinal and lateral axis and rotational movement along the yaw axis. The translation movement is similar to the xzo condition with an additional rotation on every vehicle overtake with an angle randomly selected between (30°, 150°, 210°, 330°) as in the oor,xor and ozr conditions.

Figure 1: First person view of the VR game environment.

2.3 Experiment protocol:

The experimental design consisted of eight sessions, with a minimum interval of one day (up to three days) between each session. To counterbalance the potential impact of order effects, participants always began with the "ooo" condition, which was expected to be the least sickness-inducing condition. The remaining seven conditions were randomized using a Latin-Square design. All experimental sessions were conducted in a sound-attenuated room.

At the onset of the first session, participants were asked to complete a demographic questionnaire to provide information on their gender and past experience with VR and motion sickness. Prior to each subsequent session, participants completed the Simulator Sickness Questionnaire (SSQ) as a baseline measure of their health status. During the 20-minute VR exposure, physiological measures of gastric and heart activity were continuously monitored, and the Fast Motion Sickness Questionnaire (FMS) score was recorded at one-minute intervals. The session concluded with the post-SSQ

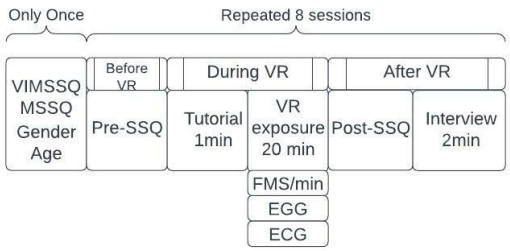

Figure 2: Experiment flow of all sessions. The VIMSSQ and MSSQ were assessed for only once before the VR experiments. Each session started with a pre-SSQ following a short tutorial and the 20 min VR exposure. During the VR exposure, the Fast Motion sickness questionnaire (FMS) was applied very minute.

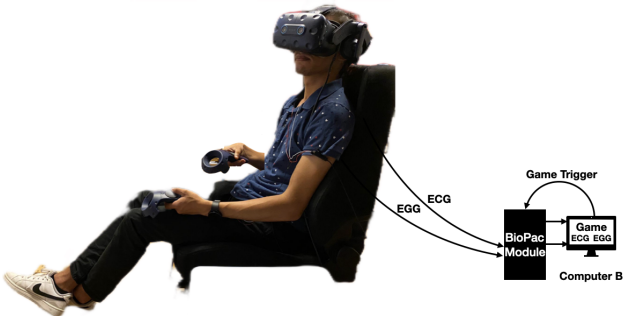

Figure 3: Settings of the experiment, participants were seated during the VR exposure. They used controllers to aim at fires on buildings

and a participant interview to gather subjective feedback on their experience, as outlined in Figure 2.

2.4 Hardware

The participant was always seated during the VR exposure (Fig. 3).

2.4.1 VR apparatus

The delivery of the Virtual Reality (VR) experience was facilitated by the HTC Vive Pro Eye (HTC, 2019). The headset was equipped with Tobii Eye Tracker units, which allowed for precise tracking of eye movements during the VR exposure. The eye-tracking data was recorded with a sampling rate of 120 Hz and boasted a level of accuracy as high as 0.5 degrees with a latency of 10 ms. The advanced HTC Vive Pro Eye headset features dual OLED screens, providing a diagonal Field of View (FOV) of 110°, a combined screen resolution of 2880 × 3200 pixels, and a refresh rate of 90Hz. The headset was powered by a 2.8GHz Intel Core i9 processor with 32GB of memory and an NVIDIA GeForce GTX 2080 graphics card, operating on a Windows 10 platform.

2.4.2 EGG and ECG

The gastric signals were acquired using the Smart EGG100D Electrogastrogram Amplifier and the MP160 System from BioPac Inc. The sampling frequency was set at 250 Hz. Two triggers, corresponding to the start and end of rotation, were sent via a parallel port from the customized VR game. The Electrogastrogram (EGG) was collected via three electrodes placed on the participant's stomach, following the standard positions recommended by BioPac (see Figure in supplementary materials). The recordings were monitored using the Acknowledge software version 5.0 from BioPac. The Electrocardiogram (ECG) signal was also collected and used to extract the breathing signal, which was necessary for the EGG data analysis.

2.5 EGG data processing

The processing of EGG signals adhered to the standardized block diagram outlined by Komorowski et al in their publication [14]. In the following sections, a comprehensive explanation of the signal processing steps will be provided.

a) Preprocessing: In the preprocessing stage, the EGG data was initially segmented based on the timestamp triggers received from the VR game. The original EGG raw data was collected at a rate of 250Hz to concurrently acquire the ECG recording, hence requiring a reduction in sampling frequency to 4Hz through downsampling. Subsequently, a Butterworth bandpass filter with a frequency range of 0.015 to 0.5Hz was applied to the down-sampled signal, followed by the application of a low-pass filter with a cutoff frequency of 0.16Hz. These filters were utilized to effectively eliminate high-frequency noise from the signal.

b) ECG-Derived Respiration (EDR):The respiratory signal, EDR, was derived from the ECG signal by first identifying the R peaks and calculating the ECG rates. The ECG signals were then formed through interpolation of the values of the normalized area under the QRS complex. The computations were carried out using the neurokit2 software. The raw EDR signals were resampled at a rate of 4Hz and filtered using a bandpass filter with a frequency range of 0.0175 to 0.5Hz.

c) Mitigation of Respiratory Disturbances in EGG Signals: During the experiment, it was observed that participants often took deep breaths when they experienced discomfort or fatigue after prolonged periods of maintaining a static posture. To address this issue, adaptive filtering was employed to effectively remove the respiratory-related noise in the signals. The adaptive filtering approach was based on the utilization of the EDR signals, as previously described, to obtain maximum correlation with the respiratory components in the EGG signals [17]. The implementation of the adaptive filtering was achieved through the use of the discrete cosine transform (DCT) and the least mean square (LMS) algorithm, as described in Liang's paper [17] and illustrated in Figure 4.

In the adaptive filtering approach, the primary inputd_j corresponds to the down-sampled EGG recordings after undergoing basic filtering, and the reference input f_j represents the down-sampled EDR signals after basic filtering. The time index, j, ranges from 1 to T, where T is the length of the signal d_j The objective of the adaptive filtering is to adjust the reference signal f_j through the use of an adaptive filter, creating a replica y_j that is highly correlated with the respiratory component of the input EGG signals [14, 17]. The adaptive filter is implemented in the transform domain using the discrete cosine transform (DCT), as transform-domain adaptive filtering has been shown to converge more effectively compared to time-domain and frequency-domain adaptive filtering [14, 17]. The weights of the adaptive filter are updated using the least mean square algorithm, in order to minimize the residual error e_j [14, 17]

Following Liang's paper [17], the reference input vector F_j is defined as:

$$F_j = [f_j, f_{j-1}.....f_{j-N+1}]^T \tag{1}$$

The DCT of reference input vector Z_j as:

$$Z_j = [z_j(0), z_j(1).....z_j(N-1)]^T \tag{2}$$

Following with the filter weight vector W_j as:

$$W_j = [w_j(0), w_j(1).....w_j(N-1)]^T \tag{3}$$

And the output of the adaptive filter y_j can be written as:

$$y_j = Z_j^T W_j \tag{4}$$

The LMS algorithm for the adaptation of the filter weights is written as:

$$w_{j+1}(k) = w_j(k) + \frac{\mu}{1/N\sum_{k=0}^{N-1}|z_j(k)|^2} e_j z_j(k) \tag{5}$$

"*where $w_j(k)$ is the k_{th} filter weight at time point j, μ is the learning rate that helps to control the convergence, N denotes the number of filter weights, and e_j is the residual error between the output of adaptive filter and the original input of d_j, e_j = d_j - y_j*" [14, 17]. The parameters for the DCT-based adaptive filter in this paper are chosen as follows: μ = 0.0001, N = 10, w is randomly generated at the beginning.

d) PostProcessing: following the standardized procedure in [14], a bandpass filter (0.015-0.5Hz) and a low pass filter (0.16Hz) were applied to the signals after the adaptive filter.

e) Running Spectrum Analysis: to extract clinically established EGG parameters, such as mean dominant frequency, dominant power, normal gastric ratio, tachy gastric ratio, and normal to tachy gastric ratio, we employed a running spectrum analysis utilizing short-time Fourier transform with a Hanning window size of 64s, in accordance with recommendations.

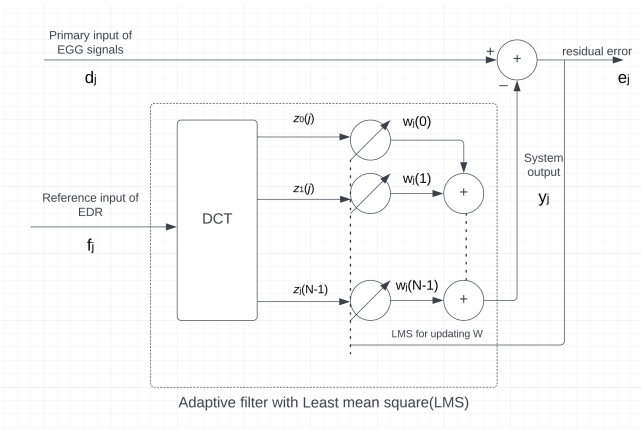

Figure 4: Overview graph of the Adaptive filter that was adopted for the treatment of EGG signals (from [17])

Following the review from Riezzo et al [2, 26, 37], we identified five essential parameters:

- **Mean dominant frequency:** the Mean dominant frequency was calculated by averaging the dominant frequency of each window size with running spectrum analysis. The dominant frequency was defined as the frequency that had the maximum power.
- **Normal gastric ratio:** "The percentage of normal slow waves can be computed from the running power spectra of the EGG. one spectrum is derived from every window size of EGG data; the minute is considered normal if its EGG spectrum exhibits a dominant power in the range of 2-4 cpm. A normal ratio above 70% is considered as the normal state in human beings." [37].
- **Tachy gastric ratio:** It is computed with the same method as the normal ratio except that the target frequency range is 4-9 cpm [37]
- **Brady gastric ratio:** It is computed with the same method as the normal ratio except that the target frequency range is 0.5-2 cpm [37]
- **Normal to tachy gastric ratio:** This ratio is calculated as (Normal gastric ratio) /(Tachy gastric ratio).

3 Results

3.1 Participants

Participants were recruited through the intranet of EPFL. Inclusion criteria stipulated that participants complied with the following rules: 1) abstain from consuming alcohol, motion-sickness medication, or similar substances for a minimum of 12 hours prior to the experiment, and 2) have their last meal at least two hours before the session. A total of 26 participants (10 female) aged between 18 to 25 (M = 21, SD = 1.9) participated in this study. Participants were compensated with cash. The study was approved by the relevant institutional review board and adhered to the ethical guidelines set forth by the associated project.

3.2 Statistical analysis

Data analysis was conducted using custom-written Python code. Normality tests were applied to determine whether the sample data were normally distributed. The Shapiro-Wilk test was used to perform the normality test. For parametric data in a normal distribution, the Paired t-test was used. For non-parametric data, the Friedman and Wilcoxon-signed rank tests were applied for post-hoc analysis. To examine the presence of a statistically significant interaction effect between three factors, a three-way repeated-measure ANOVA was used. Additionally, a permutation test was used to compare groups with different sample sizes. The strength of the linear relationship between two variables was assessed using Pearson correlation (e.g., correlation between Motion Sickness Susceptibility Questionnaire (MSSQ) and Simulator Sickness Questionnaire (SSQ)).

3.2.1 General results-SSQ

Fig. 5 shows the variation of the Simulator Sickness Questionnaire (SSQ) Total Scores (noted ΔSSQ or Delta_TS) for all conditions. Fig. 6 highlights the most sick condition for all participants. Normality distribution was examined using the Shapiro-Wilk test and the resulting p-values were calculated. The results indicated that only the "ooo" condition did not follow a normal distribution. Therefore, the Wilcoxon signed-rank test was applied for this condition, while the pairwise t-test was used for the remaining conditions. The analysis revealed that all p-values, except for the "ooo" condition, were less than 0.05, indicating that the "ooo" condition was the least sickness-inducing. The conditions with Yaw rotation induced significantly more cybersickness than those without. Specifically, the "ozr" condition was ranked as the most sickness-inducing combination, followed by "xor" and "xzr." In contrast, the "ooo," "xoo," "ozo," and "xzo" conditions induced less sickness.

3.2.2 Three-way Repeated measure ANOVA

Given the within-subject design with a repeated measure of 8 sessions, a three-way repeated measure analysis of variance (ANOVA) was performed to study the main effects and interactions of the three independent factors. The assumptions of the repeated measure ANOVA were examined prior to conducting the analysis. The Shapiro-Wilk test was used to determine whether all levels of delta total SSQ scores followed a normal distribution, and it was found that only the "xoo" condition did not. However, as the sample size was more than 25, this requirement was considered inconsequential. Secondly, Mauchly's test was conducted, and the results did not indicate any violation of sphericity. As the assumptions were met, a three-way repeated measure ANOVA was performed. The results are presented in Table 1.

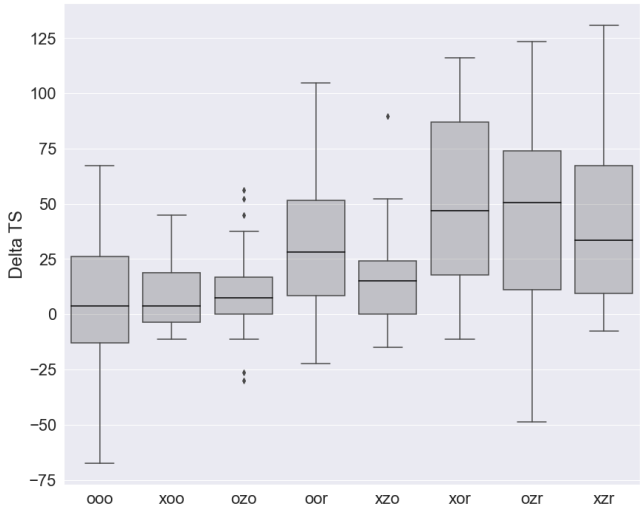

Figure 5: ΔSSQ Total means of each condition. Error bars represent the standard deviation.

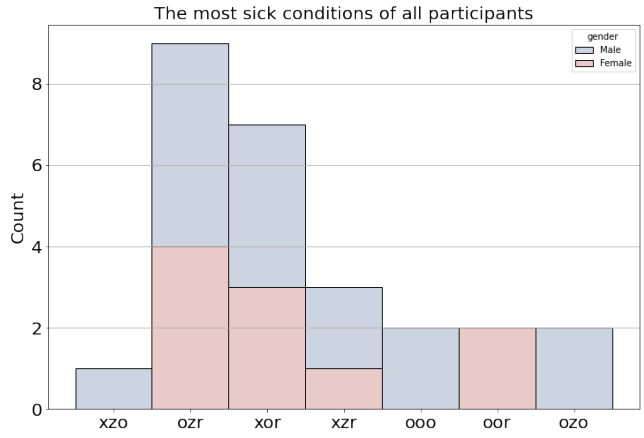

Figure 6: The distribution of the most sick condition for each individual. The Count axis presents how many participants eventually experienced the strongest sickness in the axis, grouping by Gender

3.2.3 Post-hoc analysis

The three-way repeated measure ANOVA revealed that rotation had a main effect on cybersickness, and the interaction of the three factors also had a strong effect. Therefore, pairwise post-hoc tests (parametric and non-parametric) were conducted to examine the differences. The p-values were corrected using the Bonferroni correction. The pairwise tests demonstrated that the interaction of the ZR factors and the XR factors had a strong significant effect on cybersickness, both with p-values less than 0.001. However, the result was different when considering the interaction of X*Z, with a p-value of ($p = 0.23$), further confirming the main effect of rotation. In terms of the single axis, X and Z had a non-significant effect on cybersickness ($p = 0.13$ and $p = 0.32$), while R had a strong significant impact on cybersickness ($p < 0.001$).

3.2.4 Gender factor

We further examined the effect of gender on cybersickness. As the number of participants per gender was not balanced, a permutation test was applied. The results showed that there was no significant difference between genders in general or in each condition.

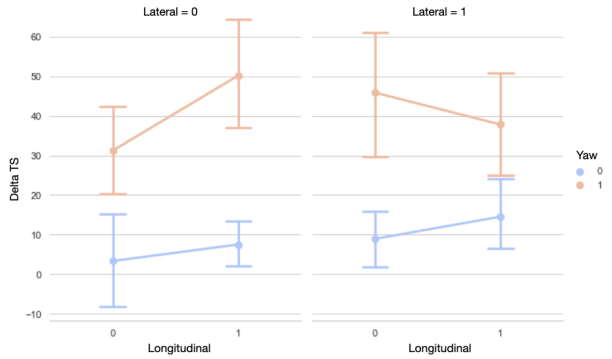

Figure 7: Three-way Anova graph, error bars represent the standard deviation.

Table 1: Three-way repeated measure Anova

Factor	F-Value	Num DF	Den DF	pr>F
X	2.36	1.00	25.00	0.137
Z	0.99	1.00	25.00	0.329
R	38.48	1.00	25.00	0.000
X:Z	2.65	1.00	25.00	0.116
X:R	0.00	1.00	25.00	0.931
Z:R	0.55	1.00	25.00	0.465
X:Z:R	9.73	1.00	25.00	0.004

3.2.5 Individual susceptibility classification with SSQ

3.2.6 Fast Motion Sickness questionnaire (FMS)

3.2.7 Correlation analysis

With regard to the correlation between MSSQ and SSQ scores, it was surprising to find that there was a weak positive correlation between MSSQ and Delta_TS (coefficient = 0.12, p = 0.04). An examination of the correlation between VIMSSQ and Delta_TS also revealed a very weak positive correlation (coefficient = 0.11, p = 0.09). These findings, along with the corresponding questionnaires and calculations, are documented in the supplementary materials.

3.2.8 Electrogastrogram

In order to evaluate the relationship between gastric activity and cybersickness, we examined the mean dominant frequency and the normal ratio of gastric signals recorded during the VR exposure. The results, as presented in Figures 13 and 14, indicated that participants exhibited a higher dominant frequency and a lower normal ratio in conditions that involved rotations, compared to those that did not. Furthermore, the addition of rotations resulted in a decrease in the normal ratio when combined with translational movement. The normal ratio was found to be negatively correlated with Delta_TS, with the ozr condition reporting the smallest normal ratio compared to the other conditions. Additionally, we also examined the tachy ratio, which is known to be a nausea indicator according to previous studies [13]. The results were consistent with Delta_TS, with ozr and xor conditions reporting the highest tachy ratio. The tachy ratio of participants in conditions with rotations significantly increased compared to conditions without rotations. Furthermore, the normal to tachy ratio, as presented in Figure 16, revealed a significant decrease in xor, ozr, and xzr conditions, indicating that the stomach activities of participants were generally stronger in these conditions, driven mainly by nausea. Participants experienced less nausea in ooo, xoo, ozo and xzo conditions.

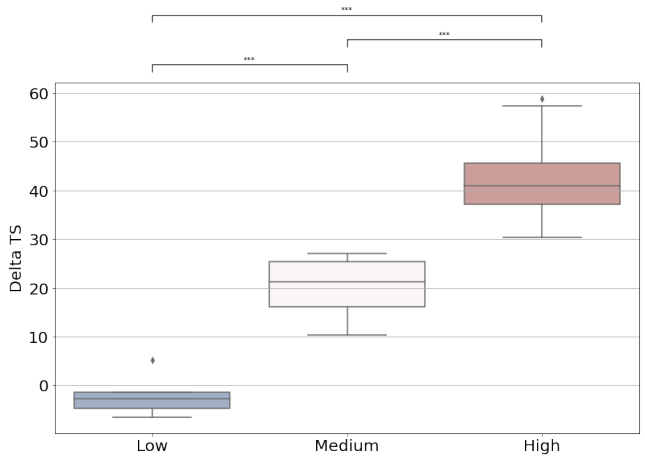

Figure 8: Results of Individual susceptibility classification by SSQ (High $>$ 30, 10 $<$ Medium $<$ 30 and Low $<$ 10 thresholds inspired by [11]), high correlational results are observed in FMS as well. We presented detailed results in the Supplementary material.

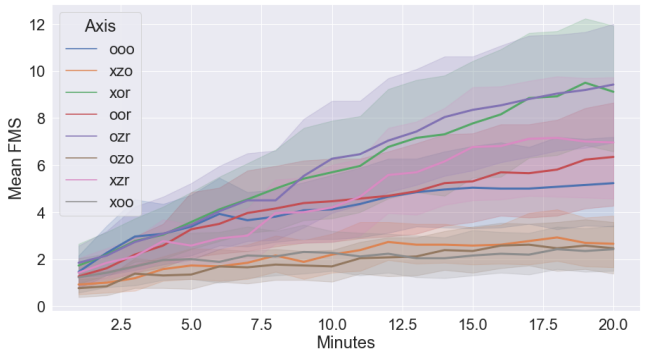

Figure 9: Descriptive lineplot of Mean FMS for each minutes (with standard deviation), colors represent different conditions,Generally, mean FMS scores exhibited an increasing trend with minutes across all sessions, but with variations in the rate of increase. It was observed that conditions xoo, ozo and xzo increased relatively slowly. These results were consistent with the SSQ findings, as conditions xor and ozr exhibited a faster increase in discomfort than the other conditions.

3.2.9 EGG with individual susceptibility

The investigation aimed to examine the correlation between susceptibility to cybersickness, as categorized by ΔSSQ scores (noted Delta_TS), and EGG parameters. The analysis specifically compared the mean dominant frequency and tachy ratio across the susceptibility groups, as illustrated in Figures 17 and 18. A comparable outcome was observed when participants were classified based on FMS scores.

The results showed that individuals with high susceptibility exhibited a higher mean dominant frequency and tachy ratio compared to those in the medium and low susceptibility groups. A one-way analysis of variance (ANOVA) was conducted to assess the differences in mean scores among the three susceptibility groups (low, medium, and high) with EGG as the dependent variable. The normality test results indicated that the data met the assumptions of normality. The one-way ANOVA revealed a significant effect of severity in Tachy ratio ($F = 6.86$, $p = 0.02$), Normal ratio ($F = 8.38$, $p < 0.01$), mean dominant frequency ($F = 8.32$, $p < 0.001$) and normal tachy ratio ($F = 1.45$, $p = 0.23$).

Given the unbalanced sample size across the groups, a permutation test was performed to determine the statistical significance of the differences. The results indicated a significant difference in mean dominant frequency between the high and low groups (p ¡ 0.001) and between the high and medium groups ($p = 0.004$). A significant difference was also found in normal ratio between the high and medium groups ($p = 0.04$) and between the high and low groups ($p = 0.03$). Furthermore, a significant difference was observed in tachy ratio between the high and medium groups ($p = 0.04$) and between the high and low groups ($p = 0.03$), with no significant difference between the low and medium groups ($p = 0.54$). Finally, no significant difference was found between normal to tachy ratio across the groups, although a trend of lower normal to tachy ratio was observed in the high susceptibility group.

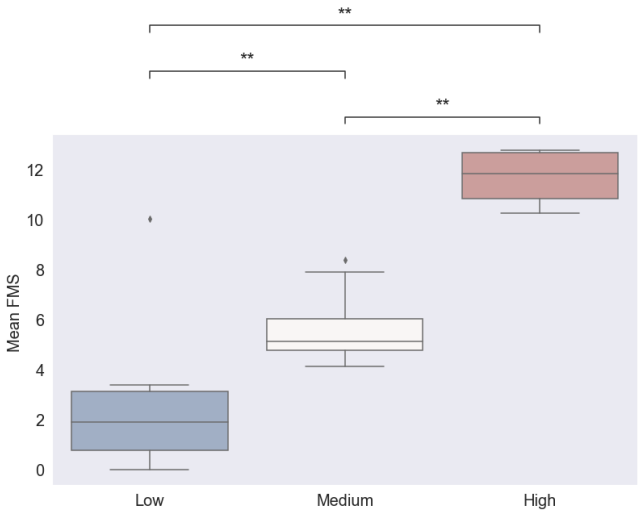

Figure 10: Individual susceptibility classfied by mean FMS of all sessions.The thresholds were adapted from Garrido et al's study [5] (Low: FMS $<$ 4, Medium: 4 $<$ FMS $<$ 10 , High: FMS $>$ 10).

3.2.10 EGG correlation with the variation of nausea (Delta_N)

The perception of nausea among individuals is subjective in nature and poses a challenge, as the same subjective rating may not necessarily correspond to an equivalent level of discomfort. To address this issue, a correlation analysis was performed between the key parameters of EGG and the Nausea subscale of the SSQ. The results revealed a medium positive correlation between the tachy ratio of the EGG and Delta_N (coefficient = 0.45, $p < 0.01$) as well as a medium negative correlation between the normal ratio of the EGG and Delta_N (coefficient = -0.31, $p < 0.001$). Furthermore, a negative correlation was observed between the normal-tachy ratio and Delta_N (coefficient = -0.36, $p < 0.001$).

Given that both the FMS and EGG were recorded during the VR exposure, a correlation analysis was also conducted between the EGG parameters and the 20th-minute score of the FMS. The results demonstrate that the correlations between the FMS and EGG are stronger compared to the correlations between the EGG and ΔSSQ. Specifically, the 20th-minute FMS score was found to be negatively correlated with the normal ratio (coefficient = -0.47, $p < 0.001$) and the normal-tachy ratio (coefficient = -0.38, $p < 0.001$), and positively correlated with the tachy ratio (coefficient = 0.44, $p < 0.001$).

4 Discussion

The results of our study indicate that the Yaw axis rotation is the primary cause of cybersickness among the three factors, with the ozr

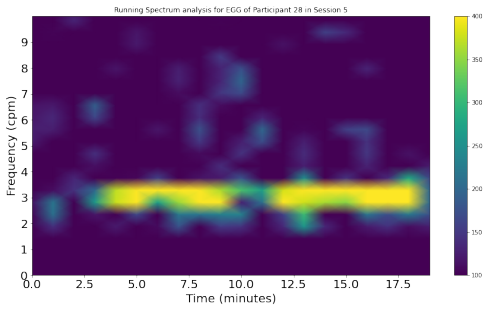

Figure 11: EGG running spectrum analysis of non-sensitive Participant A in oor condition, the EGG frequencies are mostly within the normal range

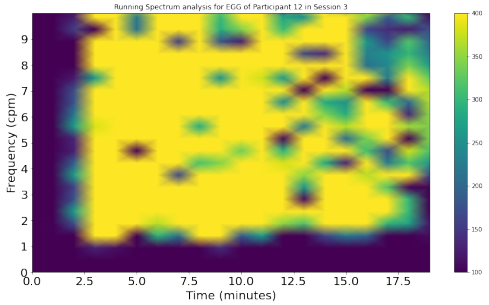

Figure 12: EGG running spectrum analysis of high-sensitive Participant B in oor condition, the EGG frequencies are shifted to tachygastria.

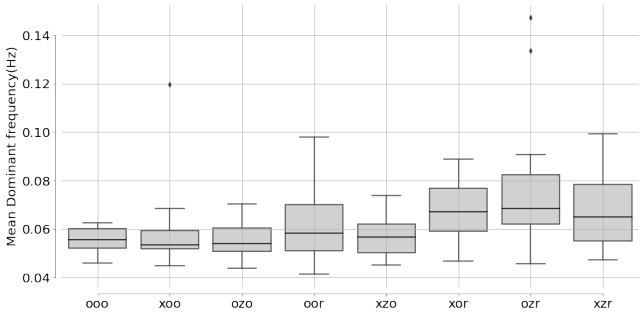

Figure 13: Results of Mean Dominant Frequency for each session

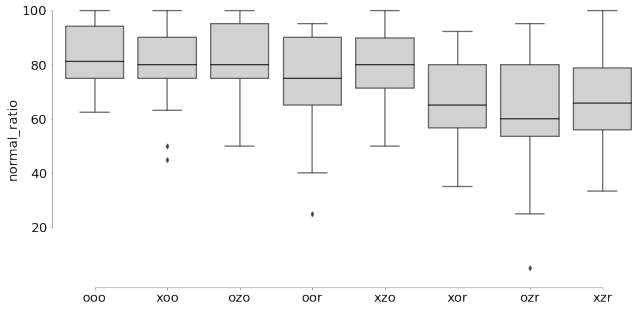

Figure 14: Results of Normal ratio for each session

condition being the worst combination. A comparison of single axes showed no significant difference between the longitudinal and lateral axes, whereas the Yaw axis rotation was found to be worse than the other two. Additionally, there was no evidence of an interaction effect or increased power when comparing the translational axes and their combinations. The ooo condition, which did not involve locomotion, was found to be the least sickness-inducing condition. However, it was noted that the mean FMS score for this condition was slightly higher than expected, potentially due to participants turning their heads more frequently or experiencing aliasing jitters in peripheral vision. Conversely, the xzr condition, which was initially expected to be the most sickness-inducing, was found to be lower than the xor and ozr conditions. This discrepancy may be attributed to a smaller proportion of rotation time in the xzr condition, due to the fixed duration of each condition.

In regards to gender, our study did not find a significant difference, which may be due to an imbalance in the number of participants of each gender. The use of a state-of-the-art HMD with eye tracking allowed for proper interpupillary distance (IPD) calibration for each individual [27], which could have minimized any potential gender differences.

Concerning individual susceptibility, low-sick or even non-sick individuals generally experienced steady levels of sickness across all conditions, while highly susceptible individuals were easily affected, particularly in conditions with rotation. Furthermore, some participants were found to be only sensitive to specific combinations of axes, while others were sensitive to several combinations.

Our results indicate that the MSSQ and VISSQ measures, commonly employed in previous literature as predictors of cybersickness, were not found to be as effective in this study. This is in contrast to previous studies that have reported strong correlations between these measures and cybersickness [6, 8, 10, 15, 34, 35]. However, our findings align with studies that have reported a lack of correlation between MSSQ and cybersickness [1, 9, 32]. The discrepancy in results may be attributed to the distinction of cybersickness from motion sickness, as discussed in [16]. Additionally, the low correlation between VISSQ and cybersickness may be due to the limited past VR experience of participants, as most of them had rarely or never experienced VR before, or the dilution of VR experience prediction power by other past experiences. These results might be explained by the fact that the VISSQ includes 11 questions, only two of which are related to VR, and that there is no weighting applied to the calculation of the final score.

In our paper, we posit that there exists a strong correlation between shifts in gastric dysrhythmias, specifically tachy and brady variations, and the onset of nausea. We provide an illustration of both a non-sensitive individual, who reported minimal sickness during the VR condition, and a sensitive individual, who experienced high levels of nausea during the VR session in figures Fig. 11 and Fig. 12, to demonstrate the range of responses to the VR environment . Through a running spectrum analysis of the EGG signals, we are able to discern the physiological changes that occur in the stomach during the onset of nausea. The results of our analysis reveal that the non-sensitive participant exhibited regular gastric activity throughout the 20-minute exposure, while in the sensitive individual, an acute frequency shift from the normal gastric rhythm to a tachy gastric rhythm was observed from the onset of the exposure.

The results of our between-conditions statistical analysis indicate that there is an increase in the tachy ratio, a finding that is consistent with previous studies in the literature (Kim et al., 2005; Koch et al., 2014). Additionally, we evaluated a comprehensive set of clinical electro-gastrographic (EGG) parameters and their correlation with cybersickness. The decrease in the EGG normal ratio, dominant mean frequency, and the increase in the EGG tachy ratio and normal-tachy ratio are indicative of nausea. This finding contradicts the

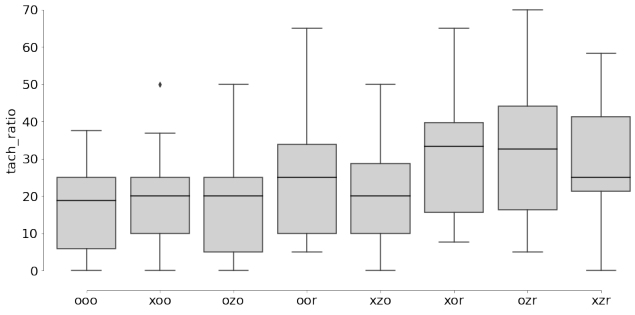

Figure 15: Results of Tachy ratio for each session

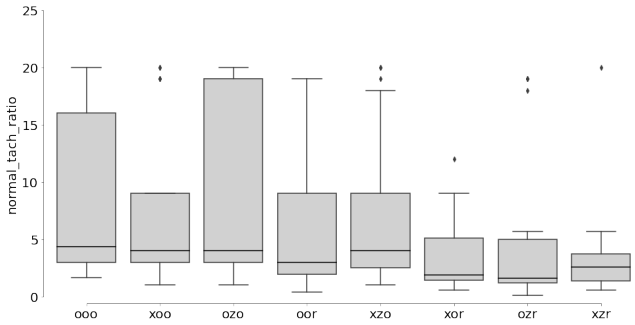

Figure 16: Results of Normal-Tachy ratio for each session

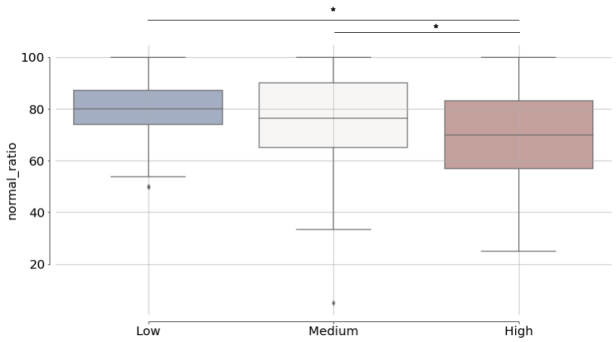

Figure 17: Results of normal ratio classified with individual susceptibility with SSQ, we added normal-tach ratio in the supplementary material

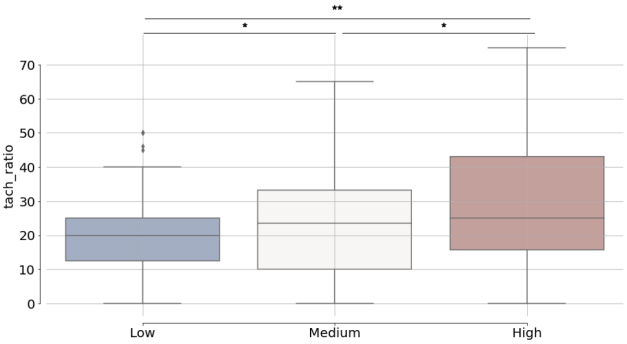

Figure 18: Results of Tachy ratio classified with individual susceptibility with SSQ, we added mean dominant frequency in the supplementary material

results reported by Dennison et al., as the brady ratio of all participants in our study was less than 5 percent (mostly 0 percent) during experimental sessions. However, we remain cautious about the results reported by Dennison et al., as previous studies have established that the brady ratio should not be the dominant ratio in healthy participants (Koch et al., 2014; Riezzo et al., 2013; Komorowski et al., 2015). Furthermore, our study is the first to examine the EGG parameters in relation to individual susceptibility, as shown in figures Fig. 17 and Fig. 18. As hypothesized, the more sensitive the participants, the higher the ratio of tachy gastria and mean dominant frequency when experiencing nausea, and correspondingly, the lower the ratio of normal gastria and the normal-tachy ratio.

4.1 Limitation and future work

Due to limitations in the study design, the sample size in the gender and individual susceptibility groups was not equitably distributed. In order to address this limitation in future research, utilizing a screening process to achieve a more balanced distribution of participants within each group would be beneficial [31]. Additionally, the current study focused on utilizing physiological signals collected from the stomach to investigate the phenomenon of nausea. However, it is acknowledged that electrogastrography (EGG) signals, while useful in measuring the intensity or changes in cybersickness, do not provide insight into the neural processes underlying these symptoms. As such, future studies may benefit from utilizing brain imaging techniques to investigate the neural mechanisms underlying the development of nausea, as well as potential interactions between the brain and gut in this process. The scope of our research is constrained in terms of the types of games and interactions investigated. To achieve more generalized conclusions, it would be beneficial to expand the study to include a wider range of games and interactions.

5 Conclusion

In this paper, we conducted a full-scale factorial design to determine the cybersickness severity to the three common navigation axes in VR games (longitudinal, lateral, and yaw). Our results show that, for individuals highly susceptible to cybersickness, Yaw was the dominant factor. However, low-sensitivity individuals were found to be immune to all factors. Furthermore, it was determined that increasing the number of translational axes did not have a significant effect on cybersickness. What was observed to be more important was the varying combinations of factors that induced cybersickness in different individuals, thus emphasizing the need to understand individual susceptibility in order to prevent cybersickness. Additionally, our results revealed that four essential EGG parameters had a strong correlation with cybersickness, three of which were newly identified in this paper. These parameters included the tachy ratio and mean-dominant frequency which had a positive correlation with nausea, and the normal ratio and normal-tachy ratio which had a negative correlation with nausea.

In conclusion, our results provide key insights into individual susceptibility to navigation axis factors. Individuals were found to have dominant factors or combinations of factors that induced cybersickness. Identifying these dominant factors for an individual is essential in order to avoid them or adopt strategies in order to mitigate their effects.

6 Acknowledgment

This research is supported by the SNF Sinergia grant CR-SII5 180319.

REFERENCES

[1] U. A. Chattha, U. I. Janjua, F. Anwar, T. M. Madni, M. F. Cheema, and S. I. Janjua. Motion sickness in virtual reality: An empirical evaluation. *IEEE Access*, 8:130486–130499, 2020.

[2] J. Chen and R. W. McCallum. Electrogastrography: measuremnt, analysis and prospective applications. *Medical and Biological Engineering and Computing*, 29(4):339–350, 1991.

[3] A. da Silva Marinho, U. Terton, and C. M. Jones. Cybersickness and postural stability of first time vr users playing vr videogames. *Applied Ergonomics*, 101:103698, 2022.

[4] M. S. Dennison and M. D'Zmura. Cybersickness without the wobble: Experimental results speak against postural instability theory. *Applied ergonomics*, 58:215–223, 2017.

[5] L. E. Garrido, M. Frías-Hiciano, M. Moreno-Jiménez, G. N. Cruz, Z. E. García-Batista, K. Guerra-Peña, and L. A. Medrano. Focusing on cybersickness: pervasiveness, latent trajectories, susceptibility, and effects on the virtual reality experience. *Virtual reality*, pp. 1–25, 2022.

[6] S. Grassini, K. Laumann, and A. K. Luzi. Association of individual factors with simulator sickness and sense of presence in virtual reality mediated by head-mounted displays (hmds). *Multimodal Technologies and Interaction*, 5(3):7, 2021.

[7] M. C. Howard and E. C. Van Zandt. A meta-analysis of the virtual reality problem: Unequal effects of virtual reality sickness across individual differences. *Virtual Reality 2021*, 1:1–26, 5 2021. doi: 10.1007/S10055-021-00524-3

[8] X. Hunt and L. E. Potter. High computer gaming experience may cause higher virtual reality sickness. In *Proceedings of the 30th Australian Conference on Computer-Human Interaction*, pp. 598–601, 2018.

[9] A. Iskenderova, F. Weidner, and W. Broll. Drunk virtual reality gaming: exploring the influence of alcohol on cybersickness. In *Proceedings of the Annual Symposium on Computer-Human Interaction in Play*, pp. 561–572, 2017.

[10] M. Kaufeld and T. Alexander. The impact of motion on individual simulator sickness in a moving base vr simulator with head-mounted display (hmd). In *International Conference on Human-Computer Interaction*, pp. 461–472. Springer, 2019.

[11] R. S. Kennedy, J. M. Drexler, D. E. Compton, K. M. Stanney, D. S. Lanham, and D. L. Harm. Configural scoring of simulator sickness, cybersickness and space adaptation syndrome: Similarities and differences. *Virtual and adaptive environments: Applications, implications, and human performance issues*, p. 247, 2003.

[12] S. Kim, S. Lee, and Y. M. Ro. Estimating vr sickness caused by camera shake in vr videography. *Proceedings - International Conference on Image Processing, ICIP*, 2020-October:3433–3437, 10 2020. doi: 10.1109/ICIP40778.2020.9190721

[13] Y. Y. Kim, H. J. Kim, E. N. Kim, H. D. Ko, and H. T. Kim. Characteristic changes in the physiological components of cybersickness. *Psychophysiology*, 42(5):616–625, 2005.

[14] D. Komorowski, S. Pietraszek, E. Tkacz, and I. Provaznik. The extraction of the new components from electrogastrogram (egg), using both adaptive filtering and electrocardiographic (ecg) derived respiration signal. *Biomedical engineering online*, 14(1):1–16, 2015.

[15] T. Kuosmanen. The effect of visual detail on cybersickness: Predicting symptom severity using spatial velocity. 2019.

[16] J. J. LaViola Jr. A discussion of cybersickness in virtual environments. *ACM Sigchi Bulletin*, 32(1):47–56, 2000.

[17] H. Liang. Extraction of gastric slow waves from electrogastrograms: combining independent component analysis and adaptive signal enhancement. *Medical and Biological Engineering and Computing*, 43(2):245–251, 2005.

[18] S. Litleskare. The relationship between postural stability and cybersickness: It's complicated – an experimental trial assessing practical implications of cybersickness etiology. *Physiology and Behavior*, 236, 7 2021. doi: 10.1016/J.PHYSBEH.2021.113422

[19] W. Lo and R. H. So. Cybersickness in the presence of scene rotational movements along different axes. *Applied ergonomics*, 32(1):1–14, 2001.

[20] P. Lopes, N. Tian, and R. Boulic. Exploring blink-rate behaviors for cybersickness detection in vr. In *2020 IEEE Conference on Virtual Reality and 3D User Interfaces Abstracts and Workshops (VRW)*, pp. 795–796. IEEE, 2020.

[21] C. MacArthur, A. Grinberg, D. Harley, and M. Hancock. You're making me sick: A systematic review of how virtual reality research considers gender and cybersickness. In *Proceedings of the 2021 CHI Conference on Human Factors in Computing Systems*, pp. 1–15, 2021.

[22] H. Oh and W. Son. Cybersickness and its severity arising from virtual reality content: A comprehensive study. *Sensors*, 22(4):1314, 2022.

[23] C. M. Oman. Sensory conflict in motion sickness: an observer theory approach. 1989.

[24] G. E. Riccio and T. A. Stoffregen. An ecological theory of motion sickness and postural instability. *Ecological psychology*, 3(3):195–240, 1991.

[25] G. Riezzo, M. Chiloiro, and V. Guerra. Electrogastrography in healthy children evaluation of normal values, influence of age, gender, and obesity. *Digestive diseases and sciences*, 43(8):1646–1651, 1998.

[26] G. Riezzo, F. Russo, and F. Indrio. Electrogastrography in adults and children: the strength, pitfalls, and clinical significance of the cutaneous recording of the gastric electrical activity. *BioMed research international*, 2013, 2013.

[27] K. Stanney, C. Fidopiastis, and L. Foster. Virtual reality is sexist: but it does not have to be. *Frontiers in Robotics and AI*, 7(4), 2020.

[28] K. Stanney, B. D. Lawson, B. Rokers, M. Dennison, C. Fidopiastis, T. Stoffregen, S. Weech, and J. M. Fulvio. Identifying causes of and solutions for cybersickness in immersive technology: reformulation of a research and development agenda. *Taylor and Francis*, 36:1783–1803, 11 2020. doi: 10.1080/10447318.2020.1828535

[29] P. Sweetser and P. Wyeth. Gameflow: a model for evaluating player enjoyment in games. *Computers in Entertainment (CIE)*, 3(3):3–3, 2005.

[30] L. Terenzi and P. Zaal. Rotational and translational velocity and acceleration thresholds for the onset of cybersickness in virtual reality. In *AIAA Scitech 2020 Forum*, p. 0171, 2020.

[31] N. Tian, P. Lopes, and R. Boulic. A review of cybersickness in head-mounted displays: raising attention to individual susceptibility. *Virtual Reality*, pp. 1–33, 2022.

[32] A. Tiiro. Effect of visual realism on cybersickness in virtual reality. *University of Oulu*, 350, 2018.

[33] L. Warwick-Evans, N. Symons, T. Fitch, and L. Burrows. Evaluating sensory conflict and postural instability. theories of motion sickness. *Brain research bulletin*, 47(5):465–469, 1998.

[34] S. Weech, S. Kenny, and M. Barnett-Cowan. Presence and cybersickness in virtual reality are negatively related: a review. *Frontiers in psychology*, 10:158, 2019.

[35] S. Weech, S. Kenny, M. Lenizky, and M. Barnett-Cowan. Narrative and gaming experience interact to affect presence and cybersickness in virtual reality. *International Journal of Human-Computer Studies*, 138:102398, 2020.

[36] C. Widdowson, I. Becerra, C. Merrill, R. F. Wang, and S. LaValle. Assessing postural instability and cybersickness through linear and angular displacement. *Human factors*, 63(2):296–311, 2021.

[37] J. Yin and J. D. Chen. Electrogastrography: methodology, validation and applications. *Journal of neurogastroenterology and motility*, 19(1):5, 2013.